ISBN: 978-3-95450-179-3 doi:10.18429/JACoW-FEL2017-WEP016

MODELING OF DIAMOND FIELD-EMITTER ARRAYS FOR HIGH-BRIGHTNESS PHOTOCATHODE APPLICATIONS*

C.-K. Huang†, H. L. Andrews, B. K. Choi, R. L. Fleming, T. J. T. Kwan, J. W. Lewellen, D. C. Nguyen, K. Nichols, V. Pavlenko, A. Piryatinski, D. Shchegolkov, E. I. Simakov, Los Alamos National Laboratory, Los Alamos, 87544, USA

Abstract

Dielectric Laser Accelerators (DLA) are capable of generating high output power for an X-ray free-electron laser (FEL), while having a size 1-2 orders of magnitude smaller than existing Radio-Frequency (RF) accelerators. A single Diamond Field-Emitter (DFE) or an array of such emitters (DFEA) can be employed as high-current ultra-low-emittance photocathodes for compact DLAs. We are developing a first principle semi-classical Monte-Carlo (MC) emission model for DFEAs that includes the effects of carriers' photoexcitation, their transport to the emitter surface, and the tunnelling through the surface. The electronic structure size quantization affecting the transport and tunnelling processes within the sharp diamond tips is also accounted for. These aspects of our model and their implementation and validation, as well as macroscopic electromagnetic beam simulation of DFE are discussed.

INTRODUCTION

DLAs can achieve acceleration gradients of GV/m in a structure that is orders of magnitude more compact than conventional metallic linacs driven by RF sources. To accelerate high current-density electron beams in DLAs, where the transverse and longitudinal dimensions of the accelerating field structure are on the order of the laser wavelength, new cathodes capable of producing small divergence, low emittance beams with dimensions matching the aperture of DLA need to be developed. DFEAs (Fig. 1), manufactured from the mold-transfer process and Microwave Plasma Chemical Vapor Deposition, are promising candidates for such a high-brightness cathode. These DFEAs consist of micron-scale diamond pyramids, together with nanometer-scale tips (Fig. 1) sharpened by an oxide layer in the mold process. DFEAs may produce tightly focused high-current bunched beams ideal for DLAs under suitable photo excitation. The effect and the required conditions of photoemission from a DFEA cathode are being studied at LANL [1].

DFEAs have already been demonstrated experimentally for the field emission [2]. Recently, DFEA field emission test is carried out at LANL with a variable anode-cathode (A-K) gap at a fixed voltage of 40 kV. The measured current is shown in Fig. 1 for the cases of most robust emission (A-K gap d < 7.2 mm, greater than ~60% emitters emit). Note the average current I per emitter may be fitted by $I \propto d^{-5.8}$, as compared to d^{-2} (d^{-m}, m~1.1-1.2) for the space-charge limited emission from a flat (sharp) metallic surface. This result indicates that the material and complex geometry/features of the DFE, as well as possible space-charge effect may play important roles in emission.

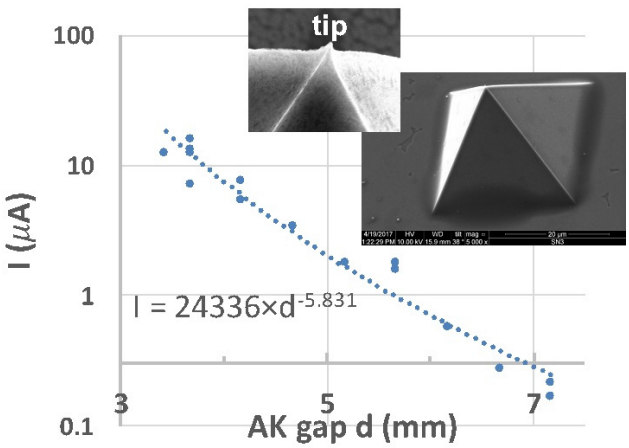

Figure 1: Averaged current (dots) per emitter as a function of A-K gap distance and their fit (dashed). The cathode has a 5×5 emitter array and each emitter has a 20 μm×20 μm base and is separated by 500 μm. Insets show the pyramid base and the sharp tip of a DFE.

SIMULATION MODEL

Since diamond is a semiconductor material (with a band gap E_g approximately 5.5 eV), its field- and photo-emission properties will depend on the charge carrier excitation (mostly electrons in the absence of impact ionization process) and subsequent transport and tunnelling processes in the emitter. Furthermore, the dielectric property of the DEFA, the geometric field enhancement at the top of the emitter and its nm-scale tip can change the field distribution over the surface. Additionally, the electronic structure size quantization effect should modify the transport and emission at the tip. A simulation model, integrating (1) carrier transport within the diamond pyramid and the surface tunnelling, (2) the quantum-size effects in the tip, and (3) the space charge effects of the emitted electrons, is essential to understand DEFA electron emission, to predict conditions favouring efficient photoemission and for the production and transport of tightly focused electron beams to a DLA. We develop such a model by combining the semi-classical MC device simulations with the electromagnetic simulations. The model components along with some preliminary results are presented below.

* Work supported by the LDRD program at LANL.
† huangck@lanl.gov

ISBN: 978-3-95450-179-3 doi:10.18429/JACoW-FEL2017-WEP016

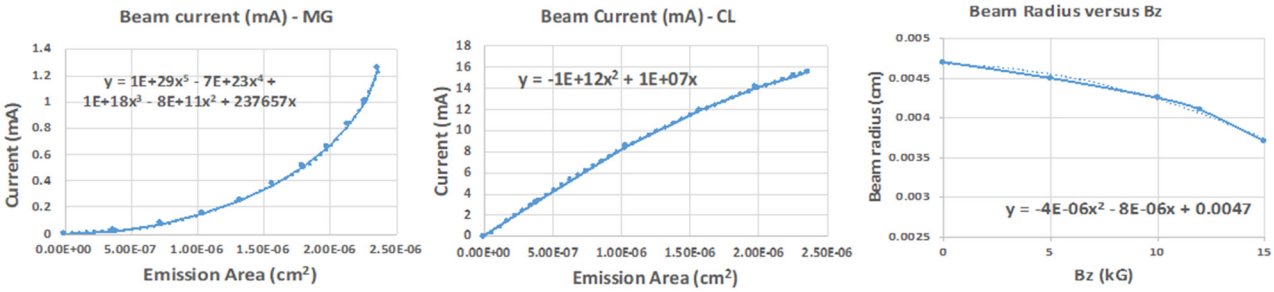

Figure 2: Simulation results using the Murphy-Good (MG, left) and Child-Langmuir (CL, middle) and their analytic fits. The right panel shows the magnetic field effect on the beam radius.

EM Simulation of Pyramid Field Emission

The fully electromagnetic relativistic code LSP was used to numerically model the electron emission process of the diamond pyramid, using the space-charge-limited and the Murphy-Good (MG) models. 2D simulations in the cylindrical (*r,z*) geometry, in which the pyramid is modelled as a cone, are used to study its emission scaling and the effect of external magnetic field on the beam size. The nm-scale tip is not modelled in the current EM simulation but will be added once our nanowire model (described below) is fully developed. The A-K gap between the base of the cone and the anode foil is set to 35 μm, and the voltage set to 0.4 kV, resulting in an electric field of 114 kV/cm at the cathode surface, similar to the experimental field strength with an A-K gap of ~3.4 mm. The simulation resolution is typically 0.5 μm and our convergence study shows it is adequate for these diode simulations. Our simulations show a significantly higher current for the space-charge-limited model in all cases. Furthermore, the current has a strong dependence on the allowed area of electron emission from the cathode surface. The simulation data and the fitted analytic forms are shown in Fig. 2. Comparison to experimental data (~12 μA/emitter) indicates that the electron emission may have occurred in a very small area (~3%) near the cone tip and is more consistent with the MG model (~1.3 mA/emitter). The effect of an external magnetic field on the electron beam trajectory are also investigated. The beam radius at 75 μm from the base of the cathode is shown in Fig. 2 with its analytic fit. The effect is only noticeable for magnetic field of 10 to 15 kG which can be challenging to implement. Design of a Pierce diode can possibly facilitate the extraction of the electron beam.

MC Model for Charge Transport/Emission

The semi-classical MC method has been widely used to model transport problems in semiconductors [3]. In the MC method, the equation of motion for charge carrier's trajectory $\boldsymbol{r}$ and crystal momentum $\hbar\boldsymbol{k}$ accounts for the energy dispersion relation. Lattice, defect and carrier-carrier scattering mechanisms can be incorporated in the resulting Boltzmann equation. Associated mean free times $\tau(E)$ are evaluated using the corresponding cross-sections. During $\tau(E)$, a carrier experiences free-flight until a random scattering event changes its momentum. At the emission surface, a carrier may tunnel through the surface potential barrier and be emitted as a free electron. The emission probability can be calculated via the Transfer-Matrix (TM) approach. This assumes a 1D electron tunnelling under a potential barrier with its profile approximated by a piece-wise function. The MC model together with the TM surface tunnelling model, have been used to study charge transport in a diamond amplifier for photocathodes. Here we adopt a similar approach for the electron transport/emission in a DEFA pyramid, while the tip will be modelled as a nanowire (NW). The photo excitation processes will be added subsequently.

Transport in the Pyramid

Our MC model employs the following simplifications: (1) In high purity diamond, the conduction band electron transport is predominantly controlled by lattice scattering. Hence, in our model, we ignore the defect and carrier-carrier scattering; (2) Both the intra-valley acoustic and inter-valley phonon scattering processes are included; (3) For intra-valley acoustic phonon scattering, a deformation potential E_1=8.7 eV is used; (4) Due to the symmetry selection rules, only the longitudinal optical (LO) phonons are allowed for inter-valley g-type (between parallel valleys) scattering. For f-type (between perpendicular valleys) scatterings, the longitudinal acoustic (LA) and transverse optical (TO) phonons are involved; (5) The g-type and f-type inter-valley scatterings are calculated for transitions between points of the energy minima with the following phonon spectrum: 0.16 eV (1900 K, LO, g3 mode); 0.13 eV (1560 K, LA, f1 mode); 0.15 eV (1720 K, TO, f2 mode).

With the above simplifications to the MC model, the electron drift velocity in the bulk diamond and its temperature dependence due to externally applied electric field is calculated and compared to available simulation result from VORPAL (Fig. 3) [4]. These results are also in good agreement with experimental measurement.

ISBN: 978-3-95450-179-3 doi:10.18429/JACoW-FEL2017-WEP016

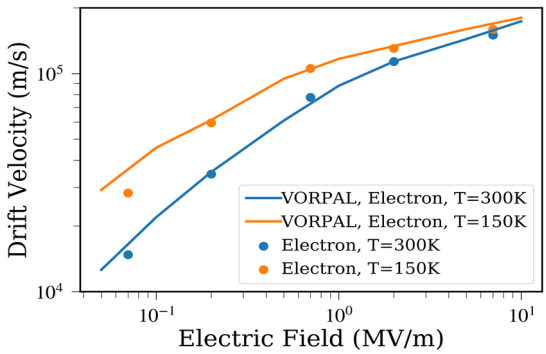

Figure 3: Electron drift velocity in an external electric field for two temperatures, T=150, 300 K. Dots are our MC results and solid lines are from VORPAL.

By combining the LSP electromagnetic simulation and the MC model, we also conduct simulation test of the electron transport in the pyramid. Figure 4 shows the longitudinal (E_z) and transverse (E_r) electric fields near the pyramid (cone) in the (r, z) LSP simulation. At t = 0, a thermal (in z direction) population of electrons at T = 300 K is initialized at the base of the pyramid (denoted by the green box in the E_z plot). The electrons' energy and longitudinal spatial distributions are shown in Fig. 4 for t = 10 ps and 30 ps. In Fig. 4, it can be clearly seen that electrons drift and diffuse as they are attracted to the top of the pyramid due to the electric field inside that is mostly longitudinal. They would gain energy in the electric field due to the drift motion, however, there is no substantial energy gain for the bulk energy distribution but a higher energy thermal tail is developed due to the scatterings.

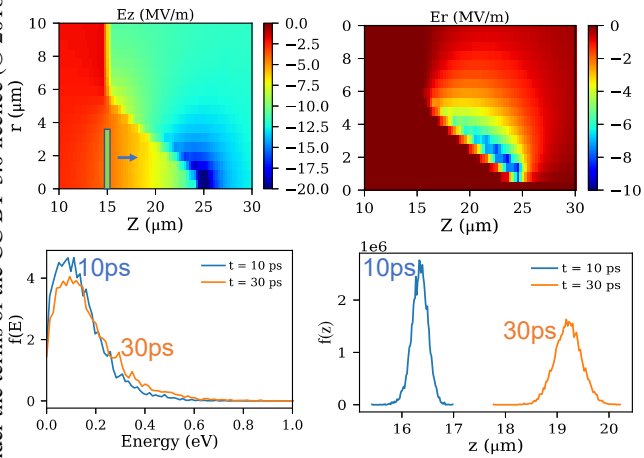

Figure 4: (Top) Electric fields inside and near a dielectric DFE pyramid with an average A-K electric field of 114 kV/cm. These fields are used to transport thermal electrons initially located at the green box. (Bottom) Electrons' energy and longitudinal spatial distributions.

Surface Emission Probability

The emission probability is evaluated by solving a 1D tunnelling problem with a spatially varying electron mass. The TM method, which treats each segment in a piece-wise surface potential profile as a constant barrier, is used to simplify the calculation. Spatial variation and anisotropy of the electron mass is considered at the crystal-vacuum interface only. Under 1D approximation, transverse momentum conservation essentially suppresses the electron emission from perpendicular valleys and also impacts the transmission from parallel valleys as shown in Fig. 5.

Tip Transport Model

To model transport via the tip of a pyramid, we approximate tip geometry by a sequence of NW segments of gradually decreasing radii (Fig. 6). Each segment is assumed to have length exceeding electron mean-free path so that Boltzmann equation can be used. Size-quantization results in a set of coupled 1-D Boltzmann equations for each energy sub-band. The coupling occurs due to the electron-phonon scattering processes. Each junction between two NW segments is accounted for via boundary condition for the Boltzmann equation.

Our scattering theory calculations show that the mismatch in the radii of NW segments at each junction corresponds to the redistribution of the sub-band population via electron forward (through the junction) scattering and back scattering, as illustrated in Fig. 6. The tunnelling outside the NW segment occurs along the tip axis at each NW junction through the interfaces with vacuum. It is to be accounted for via the TM formalism combined with our scattering theory.

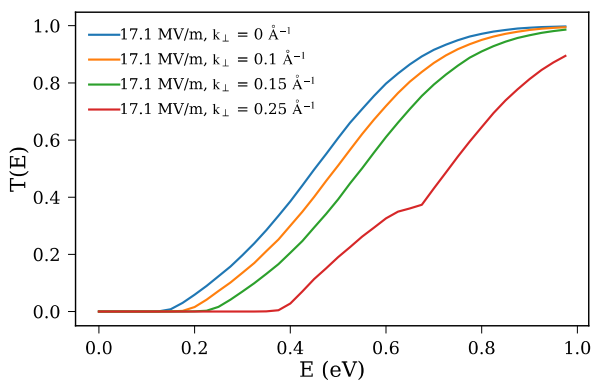

Figure 5: Energy and transverse momentum dependent transmission probability in a Fisher-type potential barrier with an external field.

ISBN: 978-3-95450-179-3 doi:10.18429/JACoW-FEL2017-WEP016

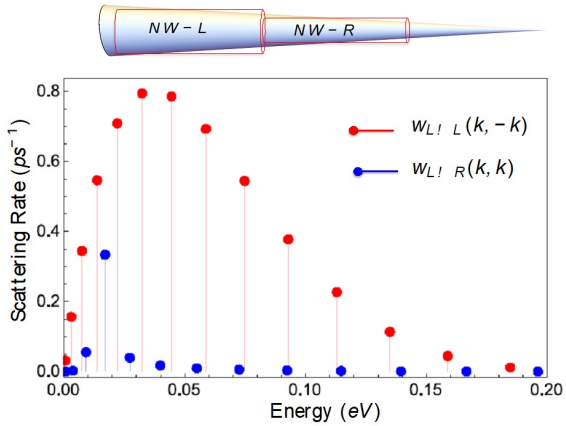

Figure 6. (Top) Partitioning of the tip into NW segments. (Bottom) Forward (L➔R) and back (L➔L) scattering rates from sub-band 4 into different sub-bands calculated for a junction between NW segments of radii 10 nm (NW-L) and 9 nm (NW-R). The electron incident kinetic energy is set to 0.2 eV and the mean-free path to 1 nm.

CONCLUSION

DFEAs are being characterized experimentally for photocathode applications relevant to DLAs and FELs. We have used electromagnetic beam simulations and are developing MC models to investigate electron transport, emission and beam dynamics issues related to the field-emission yield and the beam properties. By incorporating the NW model for DEFA tips and photo-excited electrons from electronic structure calculation, simulations will be essential for optimizing DEFA in these applications.

ACKNOWLEDGMENT

We would like to acknowledge the helpful discussions with Dr. D. A. Dimitrov and Dr. J. R. Cary regarding the diamond MC model and relevant results.

REFERENCES

[1] H. L. Andrews *et al.*, "Current experimental work with diamond field-emitter array cathodes," presented at FEL'17, Santa Fe, USA, August 2017, paper WEP015.

[2] J. D. Jarvis *et al.*, "Uniformity conditioning of diamond field emitter arrays," *J. Vac. Sci. Tech. B* 27, pp. 2264, 2009.

[3] C. Jacoboni *et al.*, "The Monte Carlo method for the solution of charge transport in semiconductors with applications to covalent materials," *Rev. Mod. Phys.* 55, pp. 645, 1983.

[4] D. A. Dimitrov *et al.*, "Multiscale three-dimensional simulations of charge gain and transport in diamond," *J. Appl. Phys.* 108, pp. 073712, 2010.